Loss of DEP-1 (Ptprj) promotes myeloproliferative disease in *FLT3*-ITD acute myeloid leukemia

Acute myeloid leukemia (AML) is a heterogeneous group of diseases caused by oncogenic transformation of hematopoietic stem and progenitor cells. Mutations in the gene encoding the tyrosine kinase FLT3 leading to internal tandem duplications (ITDs) of sequence represent one of the most frequent genetic aberrations in human AML and are associated with a dismal prognosis.[1] Herein, we show that genetic inactivation of the transmembrane (receptor-like) protein-tyrosine phosphatase (RPTP) PTPRJ/DEP-1 in FLT3-ITD knock-in mice ($FLT3^{ITD/ITD}$ mice) promotes FLT3-ITD-mediated aberrancies in hematopoiesis. $FLT3^{ITD/ITD}$ *Ptprj*$^{-/-}$ mice were characterized by enhanced extramedullary progenitor expansion, most notable in the spleen, increased colony forming unit-granulocyte monocyte (CFU-GM), and a more severe myeloproliferative neoplasia (MPN).

Our previous work demonstrated that PTPRJ/DEP-1 functions as a negative regulator of physiological FLT3 signaling, but was partially inactivated in cells expressing FLT3-ITD due to reversible oxidation by reactive oxygen species (ROS) formation.[2,3] Expression studies in human AML are also consistent with a possible contributing role of relative *PTPRJ* deficiency for FLT3-ITD driven disease. In general, according to transcriptomic data available from bloodspot, *PTPRJ* appears to be highly expressed in AML patient samples compared to progenitor cells of healthy controls (*data not shown*). Of note, the expression of *PTPRJ* appeared to be lower in FLT3-ITD positive AML compared to patient samples without ITD mutations. One data set showed a significant downregulation in the FLT3-ITD positive AML patients compared to AML patients expressing FLT3 wild-type (WT; *t*-value=-2.48, *P*=0.01).[4] In addition, the overall survival of FLT3-ITD positive patients with a low *PTPRJ* expression level tended to be shorter than the survival of patients with a high *PTPRJ* expression level (*P*=0.07, Figure 1A). The data from another study[5] revealed a similar correlation (*data not shown*). In contrast, expression of *PTPRJ* did not correlate with overall survival in FLT3 WT AML (*P*=0.21) and even showed improved survival for low *PTPRJ* expression (Figure 1B).

In order to directly study the role of PTPRJ in FLT3-ITD induced disease, $FLT3^{ITD/ITD}$ mice[6] were crossed with *Ptprj*$^{-/-}$ mice.[7] $FLT3^{ITD/ITD}$ *Ptprj*$^{-/-}$ mice showed an early onset of disease and a shortened survival (Figure 2A). The significantly reduced lifespan of FLT3-ITD mice was further shortened in response to Ptprj inactivation. The splenomegaly observed in $FLT3^{ITD/ITD}$ mice[6] appeared less pronounced in $FLT3^{ITD/ITD}$ *Ptprj*$^{-/-}$ mice (Figure 2B). While the liver weight of $FLT3^{ITD/ITD}$ mice was not significantly elevated compared with WT mice, it was significantly increased in the $FLT3^{ITD/ITD}$ *Ptprj*$^{-/-}$ mice (Figure 2C). The weight development during growth and the total weight of the adult animals did not differ among the respective genotypes (*data not shown*).

Histological spleen sections demonstrated myeloid infiltration in $FLT3^{ITD/ITD}$ mice, compared to WT or *Ptprj*$^{-/-}$ mice. This phenotype was more prominent in $FLT3^{ITD/ITD}$ *Ptprj*$^{-/-}$ mice (Figure 2E). Concomitantly, lymphocyte numbers were decreased in the peripheral blood, bone marrow, and spleen (Figure 2D,G,H; *Online Supplementary Figure S1*). While the histology of kidneys derived from $FLT3^{ITD/ITD}$ or *Ptprj*$^{-/-}$ mice was not different from that of the kidneys of WT animals, kidneys derived from $FLT3^{ITD/ITD}$ *Ptprj*$^{-/-}$ mice showed massive infiltration of leukemic cells in the renal medulla resulting in an obvious reduction of the Bowman's space around the glomerular capsule (Figure 2E). Similarly, a massive infiltration of leukemic cells was observed in the livers of $FLT3^{ITD/ITD}$ *Ptprj*$^{-/-}$ mice. Infiltration occurred predominantly around liver sinusoids, but was also widespread in the

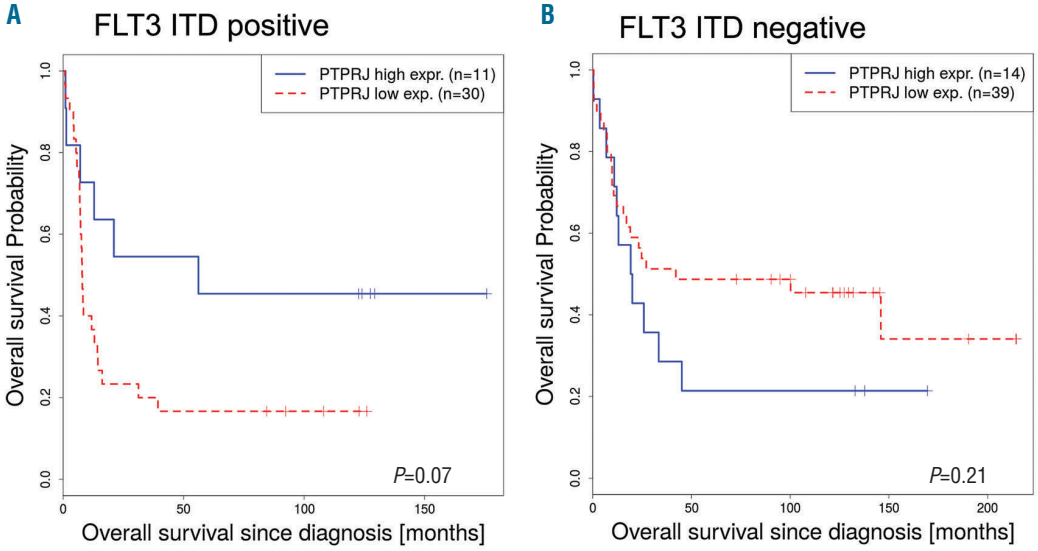

Figure 1. *PTPRJ* expression is inversely correlated to survival of FLT3-ITD positive AML patients. (A, B). Overall survival of patients (Valk study,[4,13] GEO accession GSE1159) with low (red, dotted) and high (blue) *PTPRJ* expression. Survival curves of AML FLT3-ITD positive (A: cutoff = 33.3, *P*=0.07) and FLT3 WT patients (B: cutoff = 34.9, *P*=0.21) are presented. The number of patient samples (n) is indicated.

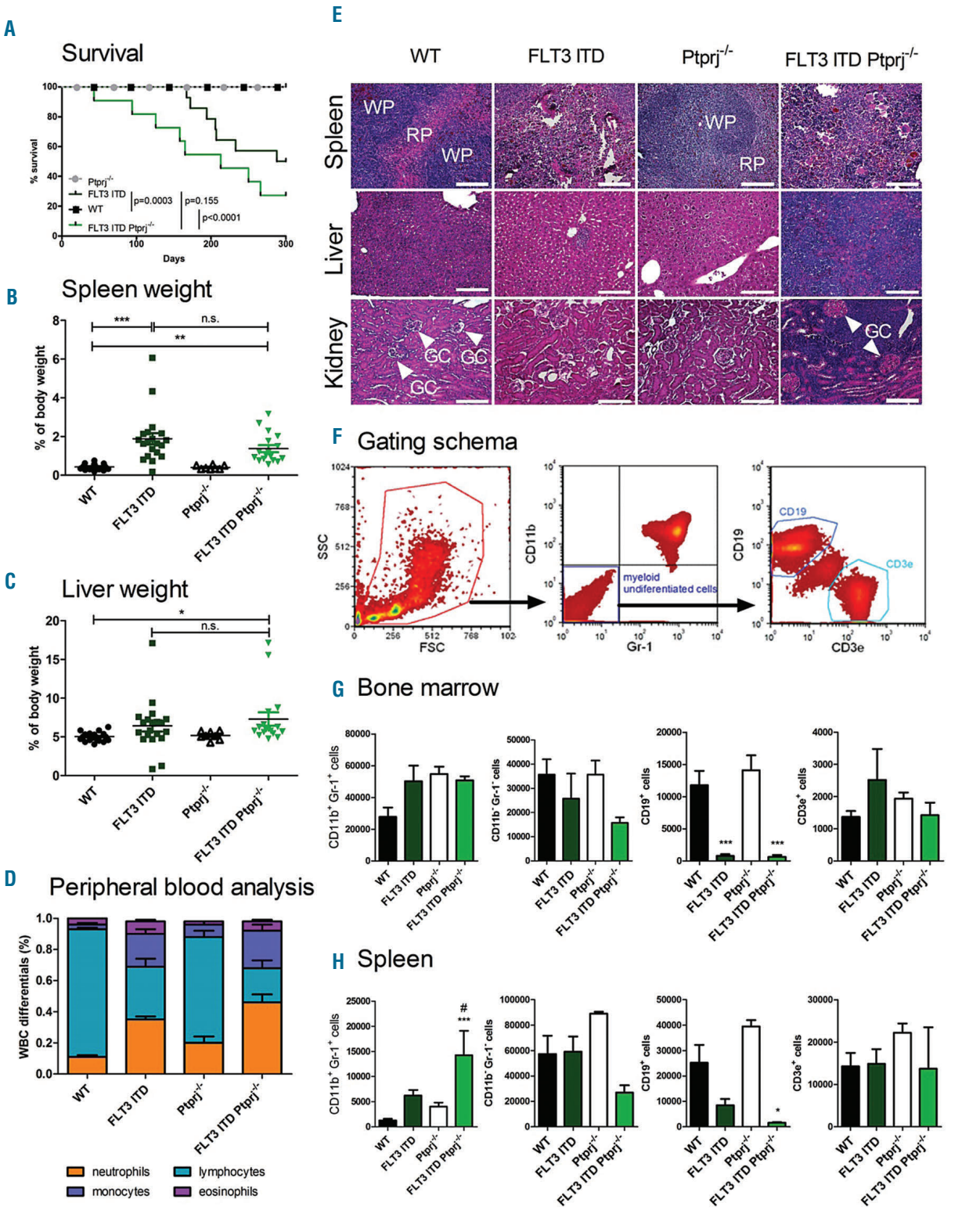

Figure 2. The inactivation of *Ptprj* results in enhanced myeloproliferation in FLT3$^{ITD/ITD}$ mice. (A) Kaplan-Meier survival curves of FLT3$^{ITD/ITD}$ *Ptprj*$^{-/-}$ and age-matched litter mates. The *P* values of the log rank test are indicated. The spleen (B) and liver (C) weight (normalized to total body weight) of 30 to 35-week-old WT, FLT3$^{ITD/ITD}$, *Ptprj*$^{-/-}$ and FLT3$^{ITD/ITD}$ *Ptprj*$^{-/-}$ mice. **P*<0.05, ***P*<0.01, ****P*<0.001 compared to WT mice. (D) White blood cell count (WBC) differentials of peripheral blood. WBC differentials are shown in mean ± SEM for FLT3$^{ITD/ITD}$ *Ptprj*$^{-/-}$ mice and controls from 30 to 35-week-old mice and indicate a reduced lymphocyte and increased neutrophil and monocyte population in *Ptprj*$^{-/-}$FLT3$^{ITD/ITD}$ mice compared to FLT3$^{ITD/ITD}$ mice. (E) H&E histopathology showing spleen (top), liver (middle) and kidney (bottom) architecture from 30- to 35-week-old WT, FLT3$^{ITD/ITD}$, *Ptprj*$^{-/-}$ and FLT3$^{ITD/ITD}$ *Ptprj*$^{-/-}$ mice (WP: white pulpa; RP: red pulpa; GC, glomerula capsule with arrows); bars indicate 100 μm. (F-H) Immunophenotype of the BM and spleen cells from FLT3$^{ITD/ITD}$ *Ptprj*$^{-/-}$ mice show an expansion of the granulocyte/monocyte population and lack of B cells. 30 to 35-week-old mice were analyzed. (F) Gating schema for the characterization of myeloid undifferentiated B and T cells (G) Graphical presentation of CD11b/Gr-1 expression in the BM (G) or spleen (H) and CD19/CD3e expression in the CD11b^{-}/Gr-1^{-} population as the total cell number out of 106 analyzed cells. Values are given as mean ± SEM; **P*<0.05, ***P*<0.01, ****P*<0.001 compared to WT; $^{\#}$*P*<0.05compared to FLT3$^{ITD/ITD}$. n.s: not significant; WT: wild-type.

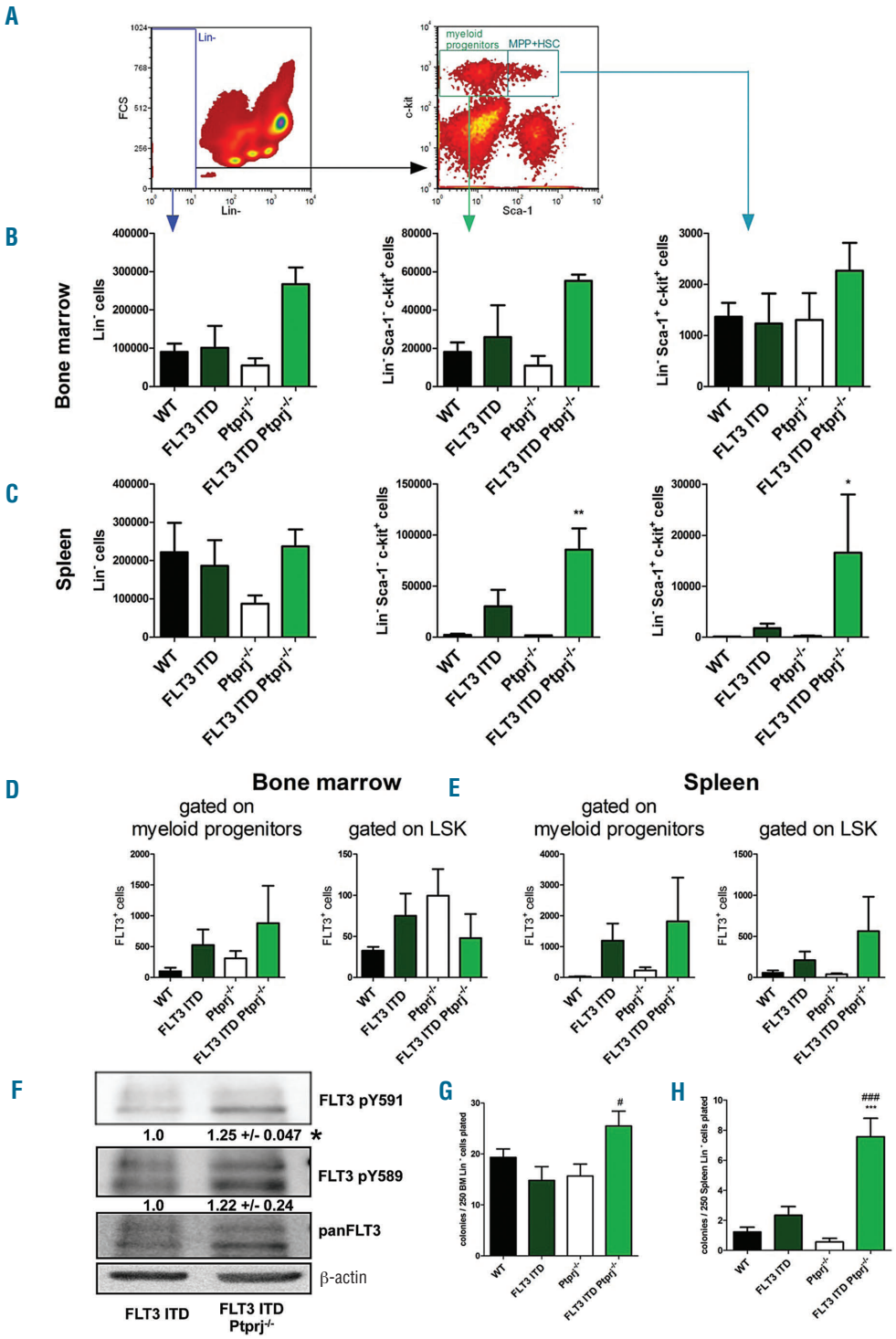

Figure 3. The inactivation of *Ptprj* in FLT3$^{ITD/ITD}$ mice affects the formation of progenitor cells. Lineage analysis of the BM and spleen cells from FLT3$^{ITD/ITD}$ *Ptprj*$^{-/-}$ mice shows an expansion of the Lin$^-$ c-kit$^+$ Sca-1$^-$ and Lin$^-$ c-kit$^+$ Sca-1$^+$ population and amount of FLT3$^+$ cells. Representative flow cytometric analysis of the BM or spleen cells derived from WT, FLT3$^{ITD/ITD}$, *Ptprj*$^{-/-}$ and FLT3$^{ITD/ITD}$ *Ptprj*$^{-/-}$ mice are shown. (A) Dot plots illustrating the gating for Lin$^-$, Lin$^-$ c-kit$^+$ Sca-1$^-$ and LSK (Lin- c-kit$^+$ Sca-1$^+$) cell populations. An abundance of these cells in the BM (B) and spleen (C) is presented. Values are given as mean ± SEM; **P*<0.05, ***P*<0.01, compared to WT. (D, E) The number of FLT3 positive cells of myeloid progenitors (Lin- c-kit$^+$ Sca-1$^-$, left) or LSK cell (right) derived from the BM (D) or spleen (E). (F) FLT3$^{ITD/ITD}$ *Ptprj*$^{-/-}$ mice show enhanced FLT3-ITD activity. Western blotting of the Lin- BM cells of 30-week-old FLT3$^{ITD/ITD}$ and FLT3$^{ITD/ITD}$ *Ptprj*$^{-/-}$ mice. BM cells were MACS-purified for Lin- immunophenotype. Cells were lysed, processed *via* sodium dodecyl sulfate polyacrylamide gel electrophoresis (SDS-PAGE) and subsequently underwent immunoblotting using phospho site specific antibodies which recognized FLT3 pY591 and FLT3 pY589. Each blot was reprobed for panFLT3 antibodies and β-actin was used as the loading control. A representative blot is presented. Numbers under the phosphor-specific blots (mean +/- SEM) represent the quantification of the phosphor-specific signals of three independent experiments, normalized to the corresponding signals with pan-specific antibodies, and relative to the signals in FLT3 ITD mice, which was set to 1.0. **P*<0.05. (G, H) The promotion of clonogenic growth of Lin- FLT3$^{ITD/ITD}$ *Ptprj*$^{-/-}$ spleen cells. Lin- BM (G) and spleen (H) cells from 30 to 35-week-old WT, FLT3$^{ITD/ITD}$, *Ptprj*$^{-/-}$ and FLT3$^{ITD/ITD}$ *Ptprj*$^{-/-}$ mice were plated on M3434 methylcellulose medium (containing stem cell factor [SCF-1], interleukin-3 [IL-3], erythropoietin [EPO]) and scored for colony formation seven days later. ****P*<0.001 compared to WT; #*P*<0.05; ###*P*<0.001 compared to FLT3$^{ITD/ITD}$ mice. WT: wild-type.

tissue (Figure 2E). Myeloperoxidase (MPO) staining confirmed the infiltration of myeloid cells in the liver (*Online Supplementary Figure S2*) and kidney (*data not shown*) of FLT3$^{ITD/ITD}$ *Ptprj*$^{-/-}$ mice in contrast to age-matched littermates of all other genotypes. Consistent with earlier findings in the FLT3$^{ITD/ITD}$ strain,[6] the number of neutrophils and monocytes in the peripheral blood of 30- to 35-week-old mice compared to their WT littermates was 3- and 6-fold higher, respectively (Figure 2D, *Online Supplementary Table S1*). This phenotype appeared even further pronounced in FLT3$^{ITD/ITD}$ *Ptprj*$^{-/-}$ animals. A white blood count (WBC) confirmed the expansion of leukocytes in this mouse strain (*Online Supplementary Figure S3A*). The red blood cell count (RBC) as well as the number of platelets of FLT3$^{ITD/ITD}$ animals was significantly reduced compared to age-matched WT littermates (*Online Supplementary Figure S3B,C*). The loss of Ptprj in FLT3$^{ITD/ITD}$ mice did not further promote this effect. In FLT3$^{ITD/ITD}$ *Ptprj*$^{-/-}$ mice hemoglobin (HGB) was significantly enhanced compared to FLT3$^{ITD/ITD}$ mice (*Online Supplementary Figure S3D*).

The previously reported increased number of mature myeloid (Gr1^{+}/CD11b^{+}) cells in the bone marrow (BM), and particularly in the spleen of FLT3$^{ITD/ITD}$ mice[6] was further elevated in the spleen and in peripheral blood in response to Ptprj inactivation (Figure 2G,H; *Online Supplementary Figure S1*) demonstrating that the absence of Ptprj may lead to the acceleration of the myeloproliferative phenotype driven by FLT3-ITD. Comparative analysis of cytospins of age-matched littermates confirmed an expanded monocyte population in the BM (*Online Supplementary Figure S3E*). In the spleen a massive infiltration of Gr1^{+}CD11b^{+} myeloid cells was observed in FLT3$^{ITD/ITD}$ *Ptprj*$^{-/-}$ mice (Figure 2H). The number of CD19^{+} cells was drastically reduced in FLT3$^{ITD/ITD}$ mice. While in the BM this reduction was irrespective of Ptprj activity, in the spleen *Ptprj*$^{-/-}$ resulted in a further abrogation of CD19^{+} cells (Figure 2G,H). The amount of CD3ε^{+} T cells of the Gr-1- CD11b^{-} population did not change in any of the investigated genotypes (Figure 2G,H). These data reveal that the inactivation of Ptprj did not promote an inflammatory phenotype in the FLT3$^{ITD/ITD}$ background and aberrancies are due to altered hematopoiesis.

To address the question whether inactivation of Ptprj in FLT3$^{ITD/ITD}$ mice affects the abundance of hematopoietic progenitor cells, lineage negative (Lin-) cells from the BM and spleen were characterized. While the single genetic lesions did not alter the number of Lin- cells in the BM, a roughly 2.5-fold elevation in FLT3$^{ITD/ITD}$ *Ptprj*$^{-/-}$ mice was observed (Figure 3B). In the spleen of *Ptprj*$^{-/-}$ mice, a reduction of about 50% of this cell population compared to WT or FLT3$^{ITD/ITD}$ littermates was detected. Previous reports have highlighted an increase of hematopoietic stem and progenitor cell numbers in FLT3$^{ITD/ITD}$ spleens.[8,9] Importantly, we found a further increase in the number of Lin^{-} Sca-1^{+} c-Kit^{+} (LSK) cells in the spleen of FLT3$^{ITD/ITD}$ *Ptprj*$^{-/-}$ mice (Figure 3C), whereas such differences were not observed in the BM. Taken together, these data demonstrate that the absence of Ptprj in FLT3$^{ITD/ITD}$ mice results in an increase of Lin- progenitor cells, which is predominantly apparent in the spleen. Further evaluation of the LSK compartment demonstrated reduced numbers of megakaryocyte erythroid progenitors (MEP) and elevated numbers of granulocyte-macrophage progenitor (GMP) cells in FLT3$^{ITD/ITD}$ mice, but this did not alter in response to the inactivation of Ptprj. (*Online Supplementary Figure S4*). The number of common myeloid progenitors (CMP) remained unchanged in all genotypes. The abundance of hematopoietic stem cells (HSC), long-term (LT) HSC and short-term (ST) HSC in Lin- Sca1^{+} c-kit^{+} cells using CD34 and FLT3 staining remained unchanged among the different mouse genotypes (*data not shown*).

The previously reported massive expansion of FLT3 positive cells[8] was confirmed in our FLT3$^{ITD/ITD}$ mouse model: in Lin^{-} c-Kit^{+} progenitors derived from FLT3$^{ITD/ITD}$ mice, a 5- or 40-fold elevation of FLT3 positive cells in the BM or spleen, respectively, was observed compared with WT mice (Figure 3D,E). The inactivation of Ptprj resulted in a further increase of this cell population (Figure 3D,E) confirming extramedullary hematopoiesis in the spleen. Similarly, FLT3-ITD expressing LSK cells in FLT3$^{ITD/ITD}$ *Ptprj*$^{-/-}$ mice were enhanced in the spleen only.

Given that PTPRJ can negatively regulate FLT3 signaling, we expected that the transformation of the signaling of FLT3-ITD in the absence of Ptprj would be enhanced, thereby promoting the myeloproliferative phenotype. To assess FLT3-ITD signaling activity, Lin- cells from the BM of 30-week-old mice were purified by magnetic-activated cell sorting (MACS) and subsequently probed for activity specific phosphorylation of FLT3. While in WT or *Ptprj*$^{-/-}$ cells the level of FLT3 expression was too low to be detected by western blotting, a significant increase of FLT3-ITD pY591 autophosphorylation activity could be detected in cells from FLT3$^{ITD/ITD}$ *Ptprj*$^{-/-}$ mice compared with cells from FLT3$^{ITD/ITD}$ mice (Figure 3F). In addition, an increased dominance of the immature FLT3 receptor of these cells further confirmed elevated activity.[10] Unfortunately, altered FLT3-ITD mediated STAT5 activation could not be demonstrated *in vivo*. Elevated kinase activity of FLT3 is known to shift the dose-response curve for tyrosine kinase inhibitors (TKI) towards somewhat lower sensitivity. Inversely, relative resistance to TKI[11] may indicate higher FLT3 signaling activity. We employed 32D cells stably overexpressing FLT3-ITD[12] with inactivated *Ptprj* using CRISPR/Cas9 (*Online Supplementary Figure S5A*). A slight elevation of pY589 site-specific phosphorylation was observed (*Online Supplementary Figure S5B*). Inactivation of Ptprj in these cells resulted in an elevated IC_{50} for the FLT3-selective TKI quizartinib (AC220) and the more broadly active TKI midostaurin (PKC412). These findings indicate that FLT3-ITD signaling activity appears to be increased upon Ptprj inactivation. Moreover, data point to the possibility that patients with lower PTPRJ levels may be relatively less sensitive to TKI treatment.

To determine the potential of progenitor cells in the BM and spleen for CFU, cells were MACS-sorted for Lin- immunophenotype and subsequently evaluated in *in vitro* clonogenic assays in M3434 methylcellulose. While the number of CFU of BM granulocytes/ macrophages of WT, FLT3$^{ITD/ITD}$ or *Ptprj*$^{-/-}$ mice showed no significant changes, the numbers of CFU-GM from FLT3$^{ITD/ITD}$ *Ptprj*$^{-/-}$ BM were significantly elevated (Figure 3G). The Lin- spleen cells of FLT3$^{ITD/ITD}$ mice formed a similar number of CFU-GM as cells from WT mice, but CFU-GMs were significantly elevated in FLT3$^{ITD/ITD}$ *Ptprj*$^{-/-}$ mice (Figure 3G). Cytospins of CFU-GM showed that cells derived from FLT3$^{ITD/ITD}$ or FLT3$^{ITD/ITD}$ *Ptprj*$^{-/-}$ BM were characterized by an accumulation of myelocytes, myeloblasts and monocytes while the abundance of granulocytes and macrophages was reduced compared to WT and *Ptprj*$^{-/-}$ littermates (*data not shown*). Almost no CFU of multipotential granulocyte, erythroid, macrophage, megakaryocyte progenitor cells (CFU-GEMM) or erythroid progenitor cells (BFU-E) were observed for all genotypes (*data not shown*). We performed the re-plating of FLT3$^{ITD/ITD}$ *Ptprj*$^{-/-}$ BM cells in order to assess for a potential gain in self-

renewal capacity by combined FLT3-ITD expression and Ptprj loss, however, FLT3$^{ITD/ITD}$ *Ptprj*$^{-/-}$ cells lacked re-plating capacity, just like the FLT3$^{ITD/ITD}$ or *Ptprj*$^{-/-}$ controls. In the absence of cytokines no colony formation of Lin- cells in methylcellulose was observed (*data not shown*).

Taken together, the inactivation of Ptprj in FLT3$^{ITD/ITD}$ mice resulted in a more pronounced infiltration of myeloid (Gr-1^{+} CD11b^{+}) cells with an increased repression of lymphocytes, which may indicate an enhanced aggressiveness of a FLT3-ITD driven disease. The expansion of the progenitor cells of FLT3$^{ITD/ITD}$ *Ptprj*$^{-/-}$ mice, most notable in the spleen, indicated an increase of extramedullary hematopoiesis. Clonogenic assays showed an enhanced CFU-GM potential of Lin- spleen cells. Moreover, the specific phosphorylation of FLT3 in Lin- BM cells derived from FLT3$^{ITD/ITD}$ *Ptprj*$^{-/-}$ mice was enhanced. Thus, our data identify PTPRJ as a suppressor of FLT3-ITD induced myeloproliferation.

Anne Kresinsky,[1] Reinhard Bauer,[1] Tina M. Schnöder,[2,3] Tobias Berg,[4] Daria Meyer,[5] Volker Ast,[5] Rainer König,[5] Hubert Serve,[4] Florian H. Heidel,[2,3] Frank- D. Böhmer[1] and Jörg P. Müller[1]

[1]Institute of Molecular Cell Biology, Center for Molecular Biomedicine (CMB), Jena University Hospital; [2]Innere Medizin II, Hämatologie und Onkologie, Jena University Hospital; [3]Leibniz Institute on Aging, Fritz-Lipmann-Institute (FLI), Jena; [4]Department of Medicine II, Hematology/Oncology, Goethe University, Frankfurt and [5]Network modelling, Leibniz Institute for Natural Product Research and Infection Biology, Hans Knöll Institute, Jena, Germany

Acknowledgments: we are thankful to Jörg Cammenga (Lund University, Sweden) for kindly providing FLT3ITD/ITD mice and Klaus Metzelder for providing additional array data. We thank Ilse D. Jacobsen for kindly providing access to the Mindray Hematology system.

Funding: the work was supported by the Deutsche Forschungsgemeinschaft (grant Mu955/11-1) and by the Federal Ministry of Education and Research (BMBF), Germany, FKZ 01ZX1302B, 01ZX1602B (CancerTel-Sys), FKZ: 01EO1002, 01EO1502 (CSCC).

Correspondence: joerg.mueller2@med.uni-jena.de
doi:10.3324/haematol.2017.185306

Information on authorship, contributions, and financial & other disclosures was provided by the authors and is available with the online version of this article at www.haematologica.org.

References

1. Papaemmanuil E, Gerstung M, Bullinger L, et al. Genomic classification and prognosis in acute myeloid leukemia. N Engl J Med. 2016; 374(23):2209-2221.
2. Arora D, Stopp S, Böhmer SA, et al. Protein-tyrosine phosphatase DEP-1 controls receptor tyrosine kinase FLT3 signaling. J Biol Chem. 2011;286(13):10918-10929.
3. Godfrey R, Arora D, Bauer R, et al. Cell transformation by FLT3 ITD in acute myeloid leukemia involves oxidative inactivation of the tumor suppressor protein-tyrosine phosphatase DEP-1/ PTPRJ. Blood. 2012;119(19):4499-4511.
4. Valk PJ, Verhaak RG, Beijen MA, et al. Prognostically useful gene-expression profiles in acute myeloid leukemia. N Engl J Med. 2004; 350(16):1617-1628.
5. Metzeler KH, Hummel M, Bloomfield CD, et al. An 86-probe-set gene-expression signature predicts survival in cytogenetically normal acute myeloid leukemia. Blood. 2008;112(10):4193-4201.
6. Lee BH, Tothova Z, Levine RL, et al. FLT3 mutations confer enhanced proliferation and survival properties to multipotent progenitors in a murine model of chronic myelomonocytic leukemia. Cancer Cell. 2007;12(4):367-380.
7. Trapasso F, Drusco A, Costinean S, et al. Genetic ablation of Ptprj, a mouse cancer susceptibility gene, results in normal growth and development and does not predispose to spontaneous tumorigenesis. DNA Cell Biol. 2006;25(6):376-382.
8. Li L, Bailey E, Greenblatt S, Huso D, Small D. Loss of the wild-type allele contributes to myeloid expansion and disease aggressiveness in FLT3/ITD knockin mice. Blood. 2011;118(18):4935-4945.
9. Li L, Piloto O, Nguyen HB, et al. Knock-in of an internal tandem duplication mutation into murine FLT3 confers myeloproliferative disease in a mouse model. Blood. 2008;111(7):3849-3858.
10. Schmidt-Arras DE, Bohmer A, Markova B, Choudhary C, Serve H, Bohmer FD. Tyrosine phosphorylation regulates maturation of receptor tyrosine kinases. Mol Cell Biol. 2005;25(9):3690-3703.
11. Tse KF, Allebach J, Levis M, Smith BD, Bohmer FD, Small D. Inhibition of the transforming activity of FLT3 internal tandem duplication mutants from AML patients by a tyrosine kinase inhibitor. Leukemia. 2002;16(10):2027-2036.
12. Grundler R, Miething C, Thiede C, Peschel C, Duyster J. FLT3-ITD and tyrosine kinase domain mutants induce 2 distinct phenotypes in a murine bone marrow transplantation model. Blood. 2005; 105(12):4792-4799.
13. Metzelder SK, Michel C, von Bonin M, et al. NFATc1 as a therapeutic target in FLT3-ITD-positive AML. Leukemia. 2015;29(7):1470-1477.